

Experimental Study on Pressure Distributions around a Circular Cylinder in the Branch of a T-junction

Yantao Yin^a, Shicong Li^a, Kai Chen^a, Liangbi Wang^b, Mei Lin^a, Qiuwang Wang^{a*}

^aKey Laboratory of Thermo-Fluid Science and Engineering, Ministry of Education, School of Energy and Power Engineering, Xi'an Jiaotong University, Xi'an, Shaanxi 710049, P.R. China

^bDepartment of Mechanical Engineering, Lanzhou Jiaotong University, Lanzhou, Gansu, 730070, P.R. China
wangqw@mail.xjtu.edu.cn

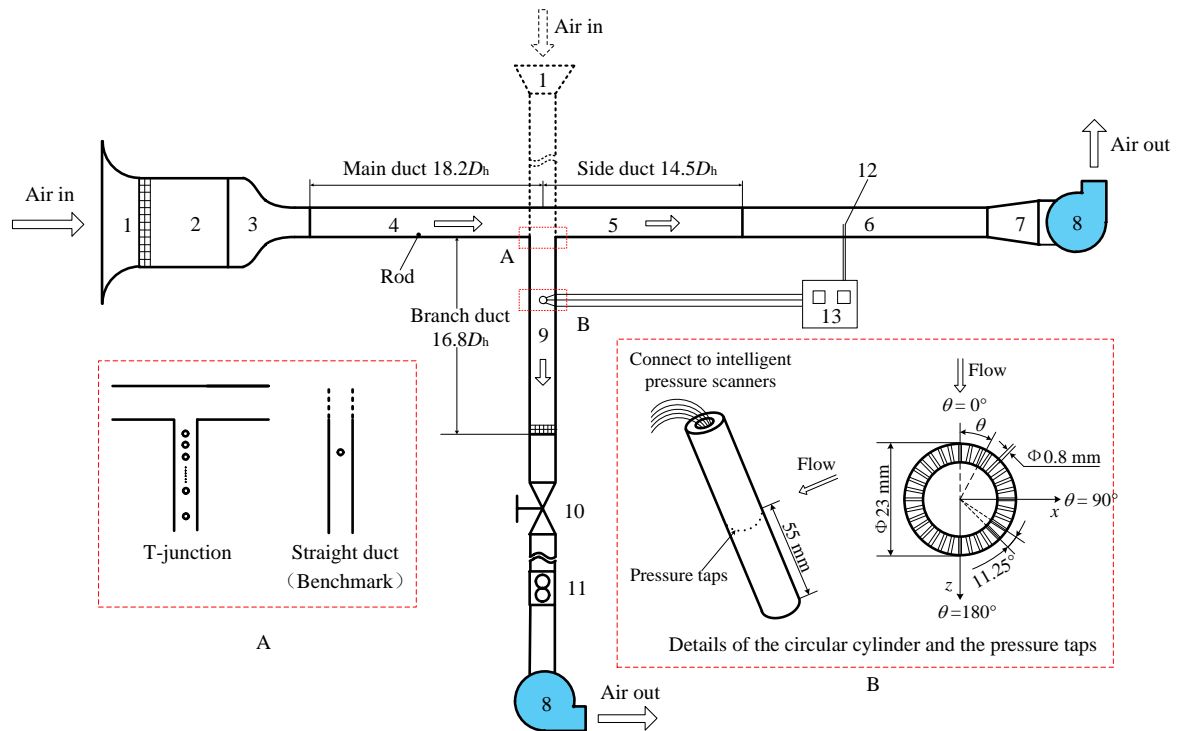
The mean pressure distributions of a single circular cylinder in the branch of a T-junction are experimentally investigated with intelligent pressure scanners (PSI 9116) in wind tunnel. Experimental data of the circular cylinder in a straight duct are conducted to provide a benchmark. Mean pressure distributions of the circular cylinder are obtained at different positions along streamwise direction under the velocity ratio (R) ranging from 0.117 to 0.614. Two dimensionless parameters including correlation coefficient (σ) and amplitude ratio (AR), are defined to analyse the pressure characteristics around the circular cylinder. In the T-junction, the pressure coefficients around a cylinder are suffered different influence at different positions, which is analysed in detail, and the level of the influence gets more and more weaken as the increase of the distance from the suction junction to the cylinder centre (z/D_h) until up to the benchmark. The change regulations of the main features included the front stagnation point, the rear stagnation point and the separation points are also presented.

1. Introduction

High speed railway plays a vital role in economic development and social progress, especially in today's China (Sun et al., 2010). Aerodynamics problems accompanied by the speed-up of train system should be urgently resolved. Ventilation is very important in the train house and the power module. The air exchange can be described as a simplified weak suction (jet) model in a T pipe junction as the velocity of the air in the ventilating device is rather small than the high speed train. The flow characteristic of weak suction (jet) takes significant effects on the drag coefficient, heat transfer efficiency, flow resistance and so on (Raghunathan et al., 2002). For flow in T pipe junction Liepsch et al. (1982) presented measurements and numerical calculations of laminar flow in a plane 90° bifurcation. The influence of Reynolds number and mass flow ratio on the velocity field, streamlines, local shear stress and pressure drop were exhibited. Neary and Sotiropoulos (1996) presented a numerical study on laminar flows through 90-degree diversions of rectangular cross-section for various Reynolds numbers, discharge ratios and aspect ratios. The flow topology patterns including zones of recirculation and streamwise vortices were exhibited. Costa et al. (2006) reported the pressure drop for the flow of a Newtonian fluid in 90° tee junctions with sharp and round corners. It was found that rounding the corners reduced the energy losses by between 10 % and 20 %. These studies mainly focus on the jet flow in T-junction. Few researches have been devoted to the suction flow in T-junction. In the present work, the pressure distributions around a circular cylinder are focused on the branch of a T-junction suction flow. Experimental studies of mean pressure distributions around a circular cylinder are conducted in the branch of a T-junction at twelve positions along the branch streamwise direction, $z/D_h = 0.5, 1, 1.5, 2, 3, 4, 5, 6, 7, 9, 11, 13$ and five velocity ratios, $R = 0.117, 0.150, 0.263, 0.439, \text{ and } 0.614$. Another one case in a straight duct are also measured to provide a benchmark. Two dimensionless parameters, correlation coefficient (σ) and amplitude ratio (AR), are proposed to analyze the pressure characteristics around the circular cylinder in T-junction.

2. Experimental system and procedure

The experiments are conducted in an open T-shape wind tunnel with two blowers running at the same time. There are two ducts included in present system, the main duct and the branch. The shape of the cross-section of the main duct and the branch are square and rectangle, respectively. Figure 1 shows the schematic diagram of the experiment apparatus. Graph A is the local enlarged main-duct/branch-interface and graph B is the details of the circular cylinder and the pressure taps. The test cylinder of 23 mm outer diameter (d) and 110 mm length (l) is vertically mounted in the branch centreline. It is made mainly of acrylic glass and has a smooth surface to neglect the influence of roughness on the flow field. Thirty-two static pressure taps of 0.8 mm diameter are equally spaced along the middle circumference of the circular cylinder. Silicon tubes with small diameter are used to connect the pressure taps and intelligent pressure scanners with precision of 0.1%. Thus we can obtain the pressure data around the circular cylinder at the same time. The two-dimensional geometric model is shown in Figure 2, with the origin located in the projection of the branch duct centre on the back side of the main duct. The circular cylinder is vertically mounted in the branch centreline, which can be moved totally 12 positions, $z/D_h = 0.5, 1, 1.5, 2, 3, 4, 5, 6, 7, 9, 11, 13$ (as shown in Figure 2). Here z refers to



1-Entrance; 2-Transition section; 3-Contraction section; 4-Main duct; 5-Side duct; 6-Flow metering duct; 7-Expansion section; 8-Blower; 9-Test section; 10-Valve; 11-Rotor flowmeter; 12- Pitot tube; 13-Data acquisition system

Figure 1: Schematic diagram of experiment system.

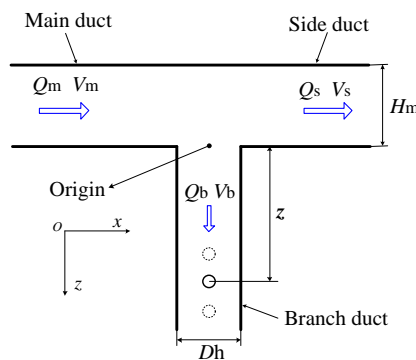


Figure 2: 2D illustration of the T-junction.

the distance from the origin to the cylinder centre and D_h refers to the hydraulic diameter of the branch duct with dimension of 110 mm. In order to compare the T-junction and the straight duct, a benchmark pressure distribution is obtained in the branch duct connected with a new entrance section, which is approximately $14D_h$ away from the branch duct entrance, as shown in Figure 1 (black dotted line). The main duct and side duct are removed from the branch duct. Thus, the T-shape junction becomes a straight duct which can provide the benchmark for the comparison with the T-junction.

In the experimental process, the air flow from the laboratory room is induced to the main duct and the branch by two frequency modulation blowers running at the same time. Here, velocity ratio, R , is given as:

$$R = \frac{V_b}{V_m} \quad (1)$$

In Eq(1), V_b and V_m refer to the bulk mean velocity in the branch duct and in the main duct inlet, obtained by a rotor flowmeter (80 - 400 m³/h) with precision of 1.5 % and a Pitot tube mounted at the flow metering duct respectively, as shown in Figure 2 and Figure 1. During the experimental process in the T-junction, the volume flow rate in the branch duct Q_b is maintained at 6.39×10^{-2} m³/s (also for the benchmark), the corresponding bulk velocity V_b is 5.28 m/s. By modulating frequency of the two blowers, five cases of velocity ratio R are examined: 0.117, 0.150, 0.263, 0.439 and 0.614.

3. Data reduction

In the present T-junction configuration, the pressure coefficient, $C_p(\theta)$, is defined as:

$$C_p(\theta) = \frac{p(\theta) - p_{\min}}{\frac{1}{2} \rho V_{bc}^2} \quad (2)$$

where $p(\theta)$ and p_{\min} refer to the pressure value at a certain angle and the minimum pressure around the circular cylinder. V_{bc} and ρ are the centreline velocity in the main duct and the density of air, respectively.

Another two parameters including correlation coefficient (σ) and amplitude ratio (AR) which measure the similarity between pressure distributions obtained in T-junction and in straight duct and describe the change level of amplitude, respectively, are defined as follows:

$$F(\delta) = \frac{\sum_{i=1}^{32} [C_p^B(\theta_i) - \overline{C_p^B(\theta_i)}][C_p^T(\theta_i + \delta) - \overline{C_p^T(\theta_i + \delta)}]}{\sqrt{\sum_{i=1}^{32} [C_p^B(\theta_i) - \overline{C_p^B(\theta_i)}]^2} \sqrt{\sum_{i=1}^{32} [C_p^T(\theta_i + \delta) - \overline{C_p^T(\theta_i + \delta)}]^2}} \quad (3)$$

$$(\theta_1 = 0^\circ, \theta_2 = 11.25^\circ, \dots, \theta_{32} = 348.75^\circ; \delta = 0^\circ, 11.25^\circ, \dots, 348.75^\circ)$$

$$\sigma = \text{Max}\{F(\delta)\} \quad (4)$$

$$(\delta = 0^\circ, 11.25^\circ, \dots, 348.75^\circ)$$

$$AR = \frac{C_p^T(\theta)_{\max}}{C_p^B(\theta)_{\max}} \quad (5)$$

where $C_p^T(\theta)_{\max}$ and $C_p^B(\theta)_{\max}$ refer to the maximum pressure coefficient of pressure distributions obtained in T-junction and in the benchmark. More details about the above parameters can be found in Wu et al. 2015.

4. Results and discussion

Figure 3 shows the typical case of the pressure distributions at different positions and the corresponding correlation coefficients and amplitude ratios under $R = 0.117$. For the benchmark, the pressure distribution curve is symmetric. It monotonically declines from 0° (front stagnation point) until to the location where the flow boundary layer separates with two minimum values occurring at 67.5° and 292.5° , between which the pressure coefficients maintain low levels and have a little minimum value at 180° (rear stagnation point). In T-junction, not enough far from the bifurcation, the pressure distribution curves are obviously asymmetry due to the highly non-uniform oncoming flow.

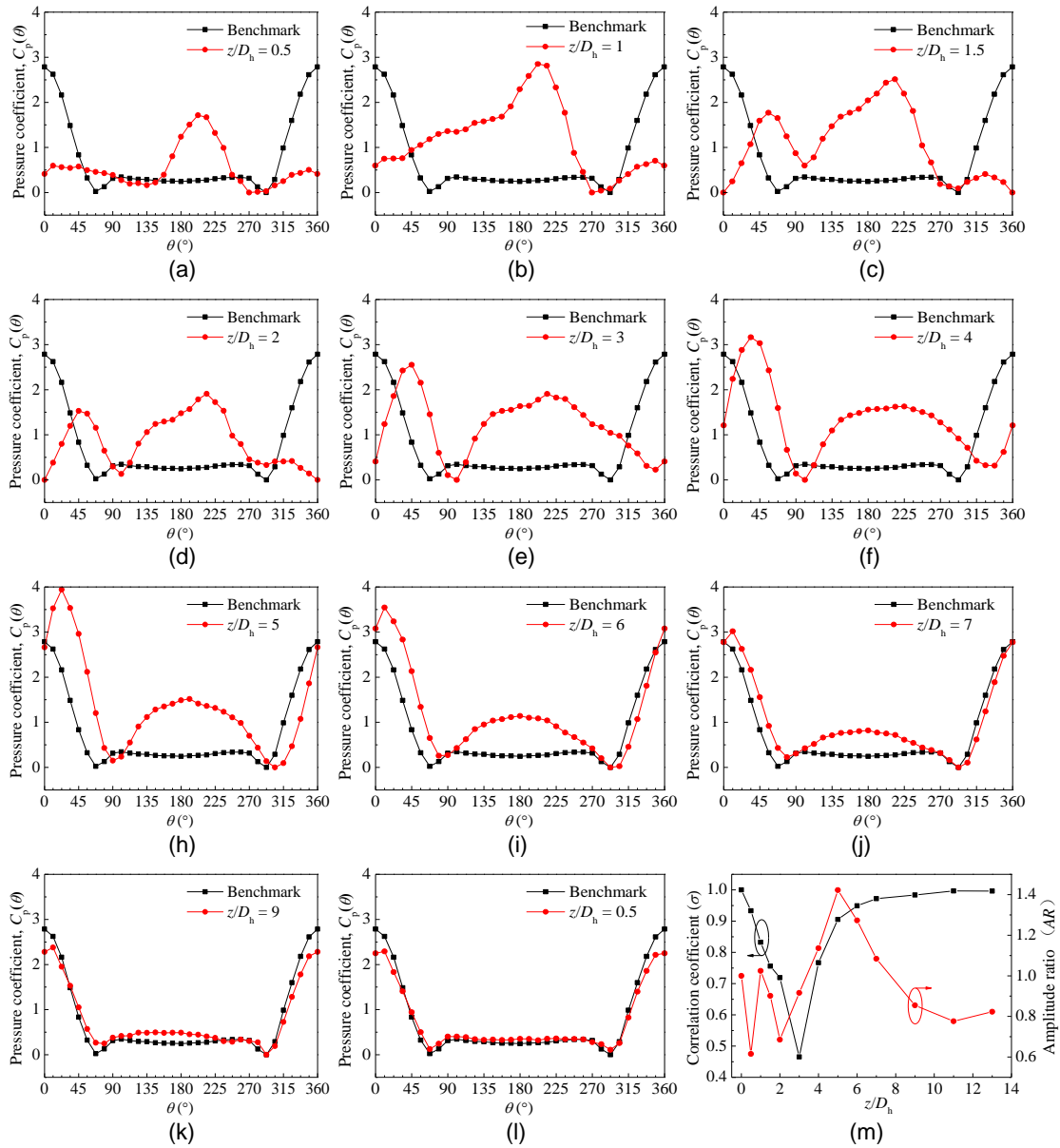


Figure 3: Pressure distributions at different positions and the corresponding correlation coefficients and amplitude ratios under $R = 0.117$.

At $z/D_h = 0.5$, one peak point occurs at about 203° and two minimum points at about 135° and 270° . The pressure coefficients from 315° to 360° and 0° to 120° change a little. The holistic pressure coefficients around the cylinder are lower than the benchmark especially at the front stagnation region. At $z/D_h = 1$, there is still one peak point at about 203° and the value is larger. Only one obvious minimum point can be seen at about 270° and the pressure coefficients increase from 0° to 203° . Also the holistic pressure coefficients around the cylinder are larger than that at $z/D_h = 0.5$.

From $z/D_h = 1.5$ to $z/D_h = 7$, double peaks and separation points are noticed and the corresponding locations show an angle shift right to the benchmark. Wu et al. 2015 reported that in the branch of T-junction two clockwise large eddies occupy most region of the duct. One is located in front of the circular cylinder, and the other behind it. The circular cylinder is located at the edges of both eddies. Thus, dynamic pressures are exerted on the circular cylinder from two almost opposite directions. That is the reason why double peaks occur in pressure distribution curves. The value at the front stagnation point is smaller than that at the rear stagnation point from $z/D_h = 1.5$ to $z/D_h = 2$, but larger at farther positions. This reflects the relative strength of the two eddies around the cylinder. From $z/D_h = 9$, the pressure distribution curve is already almost symmetric, very close to the benchmark, although some lower values exist at the front stagnation region.

As mentioned before, the main features including the front stagnation point, the rear stagnation point and the separation points appear again from $z/D_h = 1.5$ and the change regulations are analyzed as follows. At the front stagnation point, a deviation angle of about 56° gradually shifts back to 0° which is the same with the benchmark with the increase of z/D_h as shown in Figure 3, and the corresponding value of pressure

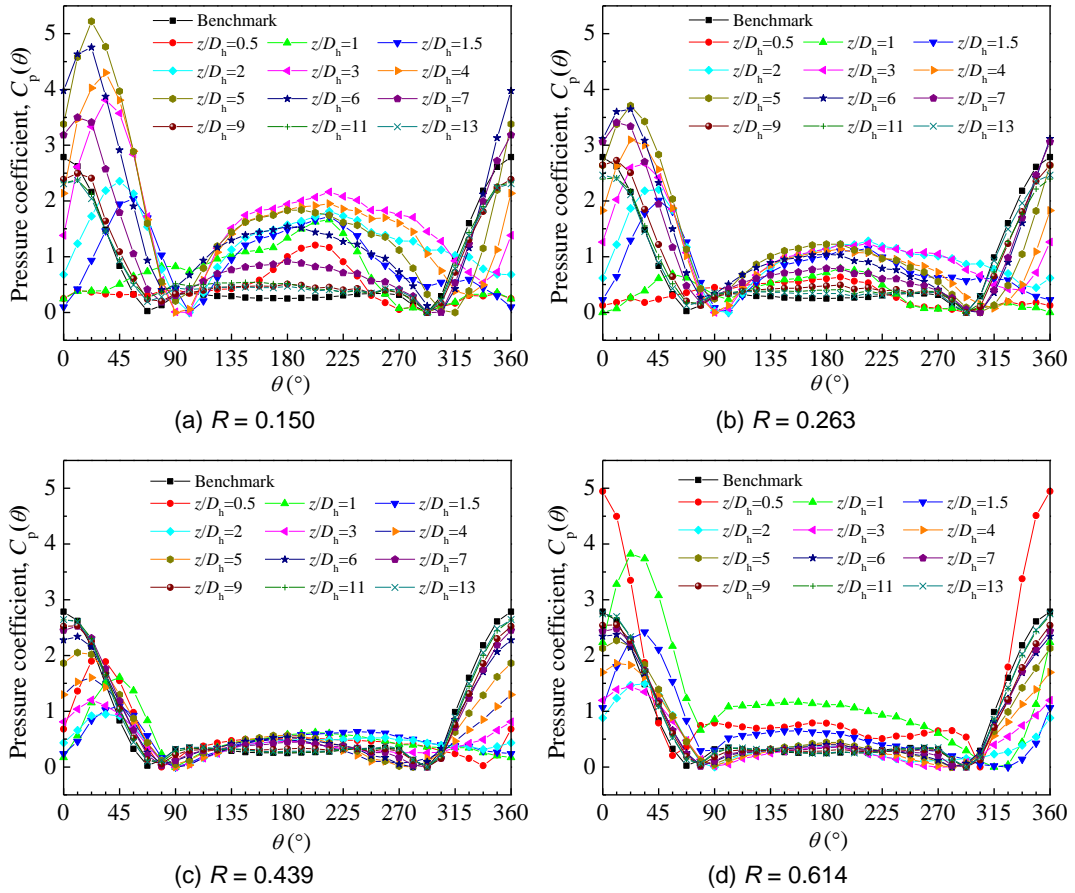


Figure 4: Pressure distributions at different positions under different R .

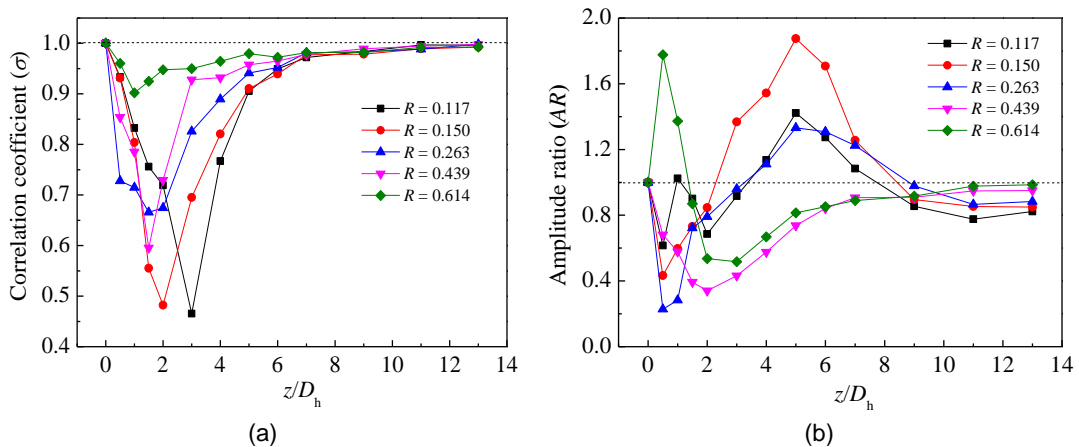


Figure 5: Correlation coefficients (a) and amplitude ratios (b) under different R .

coefficient increases first and then decreases gradually, until close to the benchmark. The two separation points are between the front stagnation point and the rear stagnation point (region) and the similar changes can be

seen. The left separation point (in Figure 3) has the shift angle from about 101° to 67.5° and the right separation point from 349° to 292.5° , although some special cases exist.

At the rear stagnation region, the peak point exists notably at about 214° from $z/D_h = 1.5$ to $z/D_h = 3$, while the pressure coefficient turns out to be more and more smooth and gentle between the two separation points at farther positions especially from $z/D_h = 9$, which position has almost the same pressure distributions with the benchmark.

The correlation coefficients and amplitude ratios under $R = 0.117$ are presented in the last graph in Figure 3. Here $z/D_h = 0$ at abscissa axis means the benchmark where both correlation coefficient and amplitude ratio equal to 1 which is for a comparison. Totally, it can be seen that the correlation coefficient decreases first and increases as the increase of z/D_h . It changes sharply near the position of $z/D_h = 3$ where has a minimum value of about 0.47 and reaches to 0.98, very close to 1 at the benchmark which can also be reflected in Figure 3 that the curve shape at $z/D_h = 9$ is very familiar with that at the benchmark. The amplitude ratio generally increases first and then decreases. It is pointed that the maximum pressure coefficient locates in the range of $\theta > 180^\circ$ from $z/D_h = 0.5$ to $z/D_h = 2$, while at the front stagnation point ($\theta < 90^\circ$) when $z/D_h > 2$, leading to some unregularly changes in amplitude ratio at these positions.

Figures 4-5 depict the pressure distributions at different positions under other velocity ratios and the corresponding correlation coefficients and amplitude ratios. Generally, with the increase of velocity ratio, the pressure coefficients present lower values in all positions around the cylinder, especially at the front stagnation and rear stagnation region, as shown in Figure 4, and the recovery to the benchmark also becomes faster, which can also be seen from the higher correlation coefficients in Figure 5 (a). At a single velocity ratio, the correlation coefficients decrease first and then increase. The positions of the minimum points are closer to the suction slot and the corresponding values are larger as the increase of velocity ratio. All the correlation coefficients are greater than 0.97, very close to the benchmark, when $z/D_h \geq 7$. For $R = 0.614$, the minimum value is already 0.9 and the pressure distribution curve is almost symmetry at $z/D_h = 0.5$. That means the changes remain similar but the influence of the suction flow on the branch duct gets more and more weakened with the larger velocity ratio. The amplitude ratios increase first and then decrease for $R \leq 0.263$ while decrease first and then increase for larger velocity ratios as presented in Figure 6 (b).

5. Conclusions

Experimental studies of pressure distributions around a circular cylinder in the branch of a T-junction are conducted. One test case in a straight duct is performed to provide a benchmark. For a single velocity ratio in the T-junction, the change regulations of the main features included the front stagnation point, the rear stagnation point and the separation points are also presented. Generally, with the increase of velocity ratio, the correlation coefficients increase. The amplitude ratios increase first and then decrease for $R \leq 0.263$ while decrease first and then increase for larger velocity ratios. For $R = 0.614$, the minimum correlation coefficient is already 0.9 and the pressure distribution curve is almost symmetry at $z/D_h = 0.5$. That means the suction effect on the branch duct is very small. The pressure distributions around a cylinder are suffered different influence at different positions, which is analysed in detail, and the level of the influence gets more and more weakened as the increase of z/D_h until up to the benchmark. That means the same with the benchmark.

Acknowledgments

We would like to acknowledge financial support for this work provided by the National Natural Science Foundation of China (Grant No. 51376145 and 51236003).

References

- Costa N.P., Maia R., Proenca F.M., Pinho F.T., 2006, Edge Effects on the Flow Characteristics in a 90 deg Tee Junction, *Journal of Fluids Engineering*, 128(6), 1204-1217.
- Liepsch D., Moravec S., Rastogi A.K., Vlachos N.S., 1982, Measurement and calculations of laminar flow in a ninety degree bifurcation, *Journal of Biomechanics*, 15(7), 473-485.
- Neary V.S., Sotiropoulos F., 1996, Numerical investigation of laminar flows through 90-degree diversions of rectangular cross-section, *Computers & Fluids*, 25(2), 95-118.
- Raghunathan R.S., Kim H.D., Setoguchi T., 2002, Aerodynamics of high-speed railway train, *Progress in Aerospace Sciences*, 38(6), 469-514.
- Sun Z.X., Song J.J., An Y.R., 2010, Optimization of the head shape of the CRH3 high speed train, *Science China Technological Sciences*, 53(12), 3356-3364.
- Wu B, Yin Y.T., Lin M, Wang L.B., Zeng M, Wang Q.W., 2015, Mean pressure distributions around a circular cylinder in the branch of a T-junction with/without vanes, *Applied Thermal Engineering*, 88, 82-93.